engineering proceedings

Proceeding Paper

Sensitivity of LH2 Aircraft Refueling to Process Parameters †

Francesco Mastropierro [1,*], Michael Quaglia [1], Enrico De Betta [1], Damiano Tormen [1], Michele De Gennaro [1] and Gianvito Apuleo [2]

[1] AIT Austrian Institute of Technology GmbH, Giefinggasse 2, 1210 Vienna, Austria; michael.quaglia@ait.ac.at (M.Q.); enrico.debetta@ait.ac.at (E.D.B.); damiano.tormen@ait.ac.at (D.T.); michele.degennaro@ait.ac.at (M.D.G.)
[2] Baykar Piaggio Aerospace S.p.A, Viale Generale Disegna, 1, 17038 Villanova d'Albenga, Savona, Italy; gapuleo@piaggioaerospace.it
* Correspondence: francesco.mastropierro@ait.ac.at
† Presented at the 15th EASN International Conference, Madrid, Spain, 14–17 October 2025.

Abstract

A preliminary analysis of aircraft refueling using liquid hydrogen (LH2) for a future short–medium-range aircraft is presented. The focus is on how selected refueling parameters influence pressure buildup and the release of boil-off gas (BOG), in order to establishing guidelines towards efficient refueling. The flow physics uses a 0-D multi-phase lump model, which accounts for the effects of the injected LH2, BOG release, heat fluxes and phase changes. Refueling is controlled by volumetric compression during the filling, and relaxation afterwards. Mass-flow profile and refueling protocol have little influence on the amount of BOG vented (~1%), but control the duration of the process, with variations close to 50%. Low initial pressure can significantly reduce the amount of BOG.

Keywords: liquid hydrogen; LH2 refueling; storage tank; boil-off gas; cross-feeding

1. Introduction

The adoption of liquid hydrogen (LH2) as fuel is a possible way to support the fundamental shift from conventional hydrocarbon fuels required for the civil aviation industry [1–3]. However, this introduces significant technical and operational challenges, introducing enormous complexity in aircraft system design, materials' selection, and thermal management [3,4]. A critical operational hurdle is the on-ground refueling process, which must be executed safely, efficiently, and remain within a timescale close to the tight turnaround times of current airline operations [5,6]. The fast transfer of large quantities of LH2 into the aircraft tanks can induce rapid pressure variation and the formation of boil-off gas (BOG), which leads to the venting of gaseous hydrogen. This is not only a loss of fuel, but also a safety and environmental hazard. Therefore, BOG management is a critical aspect of LH2 handling [7,8]. The viability of LH2-powered aircraft requires the development of efficient refueling procedures to mitigate pressure buildup and minimize BOG release.

Based on the activities undertaken by the ALRIGH2T project [9], this paper presents a preliminary study on the selected parameters of the aircraft LH2 refueling process for a short-medium-range (SMR) aircraft, which is considered a promising platform for the introduction of a LH2-based propulsion system: incoming mass-flow profile, initial fluid conditions (pressure and temperature), and an initial comparison of two refueling paradigms (parallel refueling vs. cross-feeding). The aim is to provide foundational insights

Check for updates

Academic Editors: Spiros Pantelakis, Andreas Strohmayer and Gustavo Alonso

Published: 27 April 2026

Copyright: © 2026 by the authors. Licensee MDPI, Basel, Switzerland. This article is an open access article distributed under the terms and conditions of the Creative Commons Attribution (CC BY) license.

for the development of safe, efficient, and commercially viable hydrogen refueling systems and associated procedures for the next generation of sustainable aircraft.

2. Modeling

The methodology is consistent with state-of-the art 0-D modeling for cryogenic tanks [10–12]. The thermodynamic formulation of the two-phase fluid inside the tank is presented first, with the key variables and parameters, the set of ordinary differential equations utilized, and the assumptions made due to the simplified nature of the problem and the lack of an extensive dataset for validation. The fluid model is completed by a problem-specific venting model, the description of the tank geometry and insulation properties, and the assumed mass-flow profiles for refueling. The calculations use the 0-D library HyTank [13], modified to account for cold LH2 entering the tank during refueling.

2.1. Thermodynamic Modeling

The conservation equations for mass and energy are applied to both liquid and gas volumes, whose respective thermodynamic states are assumed uniform (i.e., no stratification is included). An equation for heat exchange evaporation at the interface connects the two control volumes. The interface is approximated to a massless, infinitesimally thin layer at saturation conditions. The self-pressurization uses a Thermal Multi-Zone Model, a thermal non-equilibrium model capable of capturing the transient of boil-off. The boil-off model is a modified version of the work of Mendez-Ramos [14], and includes incoming LH2 mass flow. The environment heat input $\dot{Q}_{env}$ is distributed to the liquid ($\dot{Q}_{el}$) on the "wet" tank area and gas ($\dot{Q}_{eg}$) on the "dry" tank area, respectively. Custom heat input $\dot{Q}_{hex}$ can be added as active control. Figure 1 shows the main quantities of the thermodynamic model.

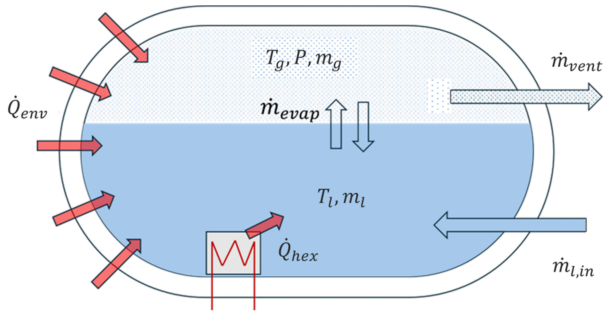


Figure 1. Control volumes and main quantities used, adapted from [10].

The mass conservation equations for the liquid (m_l) and the gas (m_g) over time are as follows:

$$\frac{dm_l}{dt} = \dot{m}_l = \dot{m}_{l,in} - \dot{m}_{evap} \tag{1}$$

$$\frac{dm_g}{dt} = \dot{m}_g = \dot{m}_{evap} - \dot{m}_{vent} \tag{2}$$

where $\dot{m}_{l,in}$ is the refueling mass-flow rate (differently from [13], signed and positive if entering the tank to account for filling), $\dot{m}_{evap}$ is the boil-off mass flow and $\dot{m}_{vent}$ is the mass flow vented via boil-off. The energy conservation equations (Equations (3) and (4)) are arranged to highlight the liquid (T_l) and gas (T_g) temperature variation over time, as in [13]. The equation for the liquid variation, modified by adding the evaporation term $-\dot{m}_{evap}h_l$, reads as follows:

$$\frac{dT_l}{dt} = \dot{T}_l = \frac{\dot{Q}_{el} - \dot{Q}_{li} + \dot{Q}_{hex} - P\,\dot{V} + \dot{m}_{l,in}h_{l,\ in} - \dot{m}_{evap}h_l - \dot{m}_l u_l}{m_l c_{p,l}}, \tag{3}$$

where $h_{l,\,in}$ is the enthalpy of the LH2 entering the tank; $\dot{Q}_{el}$ and $\dot{Q}_{li}$ are the heat fluxes from the environment to the liquid and from the liquid to the interface; and h_l, u_l and $c_{p,l}$ are the liquid enthalpy, internal energy and specific heat at constant pressure taken at T_l. No custom heat input is considered. The equation for the gas temperature variation is as follows:

$$\frac{dT_g}{dt} = \dot{T}_g = \frac{\dot{Q}_{eg} - \dot{Q}_{gi} + P\,\dot{V} + \dot{m}_g\left(h_g - u_g\right)}{m_g c_{v,g}}, \tag{4}$$

where $\dot{Q}_{eg}$ and $\dot{Q}_{gi}$ are the heat fluxes from the environment to gas and from the gas to interface, respectively. $P\dot{V}$ is the volumetric work of the liquid on the gas. h_g, u_g and $c_{v,g}$ are, respectively, the gas enthalpy, internal energy and specific heat at constant volume for a $\left(T_g, P\right)$ temperature–pressure pair. The additional equation for boil-off mass flow $\dot{m}_{evap}$ at the interface is as follows:

$$\dot{m}_{evap} = \frac{\dot{Q}_{li} + \dot{Q}_{gi}}{h_g - h_l}, \tag{5}$$

and is derived from the massless (zero internal energy) boiling-layer assumption. The layer is assumed to be at saturation temperature, which is generally different from the gas and liquid temperatures, implying non-zero heat fluxes and, thus, boil-off. Negative $\dot{m}_{evap}$ implies condensation, which can happen when a jet of subcooled liquid enters a tank with saturated ullage, or when $T_g < T_{g,\,sat}$ – the latter being unlikely during refueling due to the fast increase in pressure (and, consequently, of T_g).

Since the total tank volume is fixed and the liquid is assumed to be incompressible, the volume changes between gas and liquid are connected by $\dot{V}_l = -\dot{V}_g = \dot{m}_l/\rho_l$, where ρ_l is the liquid density. Table 1 summarizes the modeling of heat fluxes. Convection models with Newton's law of cooling and simple empirical correlations are deemed sufficient for a preliminary tool. Future developments of the code will implement more refined models, such as those proposed in [15,16].

Table 1. Types of heat-flux variables.

Heat Flux	Model Type	Heat-Transfer Coefficient	Values
$\dot{Q}_{li}$	Natural convection	Nusselt and Rayleigh [17]	Cn = 0.0135, n = 0.25 [13]
$\dot{Q}_{gi}$	Natural convection	Nusselt and Rayleigh [17]	Cn = 0.27, n = 0.25 [13]
$\dot{Q}_{el}$	Empirical	Eq. 4.56 Keller et al. [18]	MLI (see below)
$\dot{Q}_{eg}$	Empirical	Eq. 4.56 Keller et al. [18]	MLI (see below)

2.2. Venting Model

During refilling, the liquid does work on the gas, reducing its volume and increasing its pressure. Venting is required to release GH2 and prevent excessive pressure buildup. When the tank pressure reaches the venting threshold P_{vent}, a valve opens until the pressure reaches an operating pressure P_{op}. The pressure levels are indicative, as there is a trade-off between tank weight and the vented gas, which is not explored here. For simplicity, the valve effect is included in Equation (6) for the vented mass flow during refueling:

$$\dot{m}_{vent} = 0.07\left|\dot{m}_{l,in}\right|\sqrt{P_{vent} - P_{atm}}\;FL \tag{6}$$

The fill level FL is the fractional height of the tank volume occupied by liquid and P_{atm} is the ambient pressure. Equation (6) does not consider dormancy venting, since the timescale of the refueling is much shorter (minutes vs. hours).

https://doi.org/10.3390/engproc2026133045

2.3. Geometry and Insulation

Only the LH2 tanks are sized in this work. Two identical, connected tanks are considered for redundancy. Their sizing relies on very approximate assumptions, since an LH2-powered aircraft is very far from mature design. A reasonable starting point is to assume the same tube-and-wing layout, fuselage diameter and fuel energy of the A320 (chosen as representative SMR). Scaling the maximum fuel weight with the energy density of LH2 yields a capacity of 3.6 tons of LH2, corresponding to a volume of ~50 m^3 per tank (3.5 times larger than existing A320). The tanks will likely be installed at the rear of the fuselage; consequently, each tank features a cylindric main body (2.86 m length) sided by two hemispherical endcaps (3.7 m internal diameter) for combination of good gravimetric index and insulation performance. No other tank features are modelled. Importantly, impacts on aircraft design and performance are considered out of scope. The tanks are in aluminum, to combine lightness and mechanical properties. The insulation consists of a 2 cm vacuum (1×10^{-6} torr pressure) and a multi-layer insulation (MLI) with 57 layers, involving 30 layers/cm, as in [13]. The solid and gas conduction parameters are 89.8×10^{-9} and 1.46×10^{4}, respectively, derived from Eq. 6.2 and 6.3 of Keller [18]. The radiation coefficient is 5.39×10^{-10} and the emittance is 0.031. The insulation provides an environment specific heat input of ~1.5 W/m^2, in line with existing state-of-the-art insulation [19].

2.4. Refueling Conditions

All calculations assume that refueling starts at 15% *FL* and ends at 95% *FL*. The default tank's initial pressure is 1.4 bar, to avoid external gas contamination. Saturation conditions are assumed for both the liquid and the gas at t = 0, i.e., a temperature of 21.5 K. The refueling mass flow is described in Equation (7) by a canonical logistic curve profile, realistic with respect to classical pump commands and control strategies:

$$\dot{m}_{l,\,in}(\,t) = \dot{m}_{max}\left(\frac{1}{2}\left(1 + tanh\left(\frac{(t - t_{in})R_{in}}{2\pi}\right)\right)\right) - F_{out}(t - t_{out}) \quad (7)$$

where $\dot{m}_{\mathrm{l,max}}$ is the maximum mass flow achievable, R_{in} = 5 min^{-1} the pump reactiveness, and t_{out} is the time at which pump derating is applied. This profile is smooth and derivable also at t = 0, which helps its implementation in complex models. However, its formulation is a physics-educated assumption coherent with a pressure-based loading of the tank, as in [10], considering that no known aviation-specific refueling profile is available. The derating function $F_{out}(.)$ in Equation (8) controls the last part of the refueling ($FL > 75\%$), where most of the venting happens:

$$F_{\mathrm{out}}(t) = \dot{m}_{\mathrm{l,max}}(1 - \exp(-R_{out}t)H(t)) \quad (8)$$

R_{out} is the derating rate and $H(.)$ the Heaviside step function.

Four mass-flow profiles are considered, as shown in Figure 2:

- Purple (control case): lower peak mass flow, no derating—fills the tank in 35 min, for a turnaround time of ~60 min, which is closer to forecastable technology.
- Red: very high peak mass flow, no derating—fills the tank in 15–20 min, for a very ambitious turnaround time of ~30–40 min, which is closer to current SMR operations.
- Blue: very high peak mass flow and slow exponential derating.
- Green: very high peak mass flow and fast exponential derating.

https://doi.org/10.3390/engproc2026133045

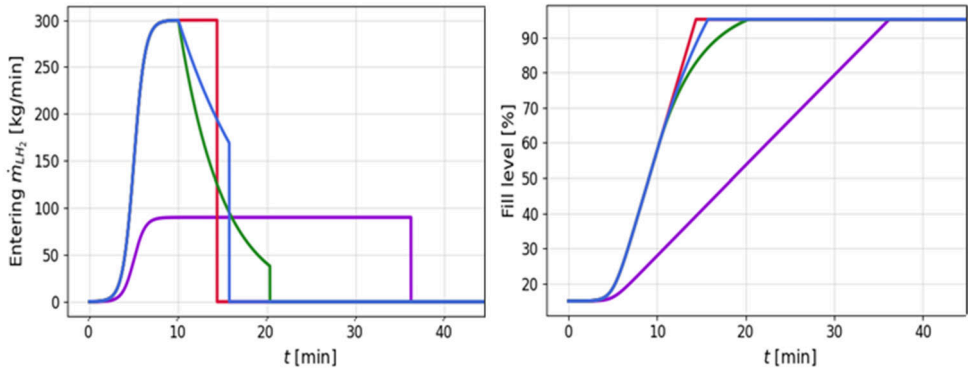


Figure 2. Inlet mass-flow profiles considered (**left**) and volumetric fill level progression (**right**).

Additionally, two refueling paradigms are also considered: parallel refilling and cross-feeding. In parallel refilling, both tanks are filled at the same given liquid mass flow. Cross-feeding assumes that one tank is filled first, to a given *FL*, then a valve opens, keeping the first tank at constant *FL* but feeding the second tank. After the second tank reaches the target *FL*, a final parallel refueling sequence for both tanks is performed.

3. Results

3.1. Sensitivity to Mass-Flow Profile

Figure 3 presents the results of the pressure variation for the four inlet mass-flow profiles. The initial pressure increase is dominated by the volumetric work, while the oscillations are due to venting, which never appears before 70% FL. After the refueling is completed, venting stops and pressure relaxation is observed, which is due to the temperature-driven heat fluxes through the interface. The time evolution of the gas temperature is similar to that shown in Figure 4 (bottom). The total amount (i.e., time integrated) of vented GH2 for a single tank is around 64.8 kg, i.e., 1.8% of the stored mass. The four profiles show a negligible relative difference in terms of vented gas (below 0.5%), with the "high mass flow" ones having an operational advantage in terms of required time. No strong trend for mass-flow rate or derating is noted; however, this may be due to the model assumptions and/or accuracy, the assessment of which requires more detailed analysis.

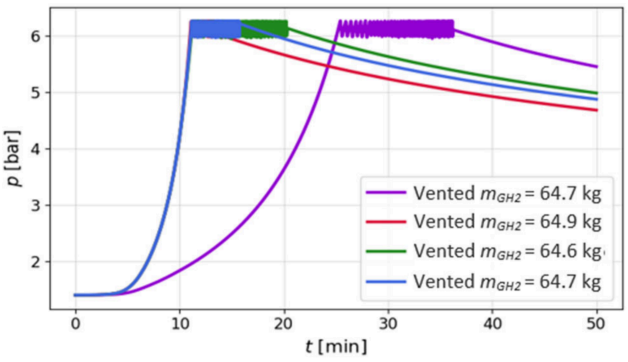


Figure 3. Effects of inlet mass-flow profiles on tank pressure and vented gas (in legend).

3.2. Sensitivity to Fluid Initial Conditions

Figure 4 shows the effects of changing the tank's initial conditions for the control case in Section 2.4 (purple). Lowering the initial liquid temperature (subcooling) by 3 K slightly reduces the amount of vented gas by 1% (0.8 kg) for an initial pressure of 1.4 bar.

https://doi.org/10.3390/engproc2026133045

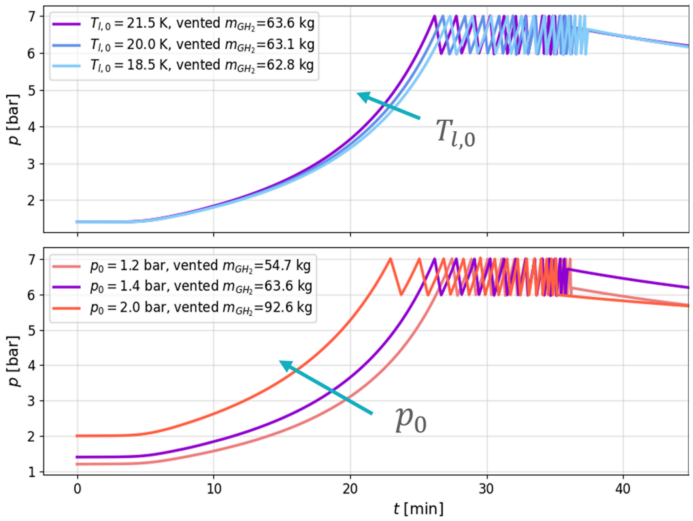


Figure 4. Effect of initial liquid temperature (**top**) and pressure (**bottom**) on pressure build-up.

Considering the short timescale of the refueling, the main driver for the reduction is the change in volumetric work. Another contributor is the lower evaporation rate (see Equation (5)), which decreases pressure buildup and GH2 mass and acts across longer timescales. This supports the use of subcooled LH2 to reduce evaporation and venting. This effect is stronger with a lower initial FL.

Changing the initial pressure significantly influences the BOG released and the onset of venting. A reduction down to 1.2 bar reduces the amount of BOG by 14% (54.7 kg), while an increase to 2 bar results in an increase of 45% (92.6 kg) and consequent early venting, in line with the considerations made by Mangold [6]. Changes in initial pressure also alters the initial temperature of gas and liquid because of the saturation hypothesis.

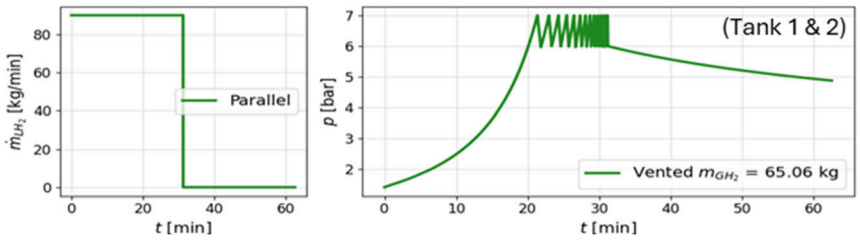
3.3. Preliminary Assessment of Cross-Feeding

Cross-feeding explores the operational context where refueling is performed at one access point for the entire fuel system, and also investigates the effect of pressure and temperature relaxation after the refueling to reduce the venting. Three paradigm scenarios are presented: "parallel refilling", where the two aircraft tanks are fed simultaneously (Figure 5a) and two cross-feeding alternatives, where tanks are first fed alternately up to 50% and 75% *FL* (respectively, Figure 5b and 5c), and then the remaining part is filled by a parallel refilling at lower mass flow. The maximum mass flow allowed inside one tank is the same as for the control case in Section 2.4, (i.e., compatible with a refilling of ~30–35 min, if kept constant), with the initial ramp-up excluded to facilitate the comparison between paradigm scenarios, given its negligible impact on BOG.

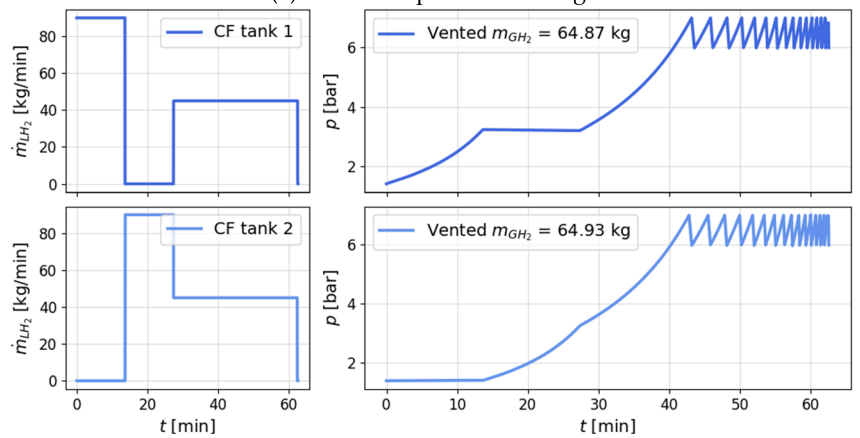
Cross-feeding reduces the amount of vented BOG by 0.4% circa (129.8 kg at 50% or 129.6 kg at 75%), compared to parallel filling (130.1 kg). The driver for the difference is the interfacial heat flux that acts for a longer time and cools down the gas. The effect of the compression work of the liquid on the gas is identical across the scenarios considered, as it acts across a much shorter timescale. Differences between different *FL* switches are marginal, resulting from the combination of the time (and pressure) at which relaxation occurs and the interfacial heat flux. Cross-feeding becomes less advantageous as average mass flow increases, as relaxation acts for less time.

From an operational perspective, cross-feeding takes twice the time of parallel filling under the set of current assumptions, but requires a smaller pump or a single access point for the entire fuel system, which is a crucial design feature. This means that the choice

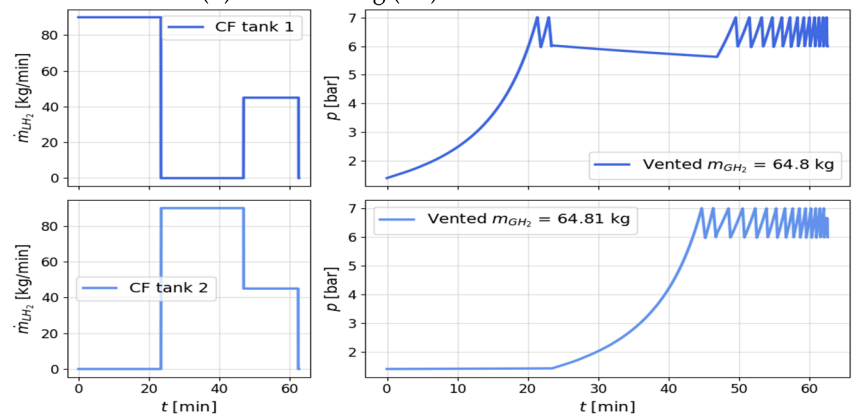
between the paradigms is more dictated by the fuel system layout and operational criteria rather than by the tank thermodynamics.



(**a**) Baseline—parallel refilling.



(**b**) Cross-feeding (CF) at 50% *FL* for tank 1.



(**c**) Cross-feeding (CF) at 75% *FL* for tank 1.

Figure 5. Results of cross-feeding paradigms.

4. Conclusions

A set of preliminary 0-D analyses is performed to study the impact of selected process parameters (mass-flow profile, tank initial pressure and temperature, and tank feeding strategies) for the LH2 refueling process for future SMR civil aircraft. The main objective is to quantify the amount of BOG vented during the refueling, to envisage strategies for its minimization. The results indicate that mass flow, initial temperature and feeding strategies cause the amount of released BOG to vary by ~1%, while low initial pressure can greatly reduce the amount of BOG. The tank thermodynamic is controlled by the volumetric work of compression during the initial refueling, and by the relaxation of gas and pressure after; venting takes place in the last phase of the refueling according to specified pressure thresholds. The average mass flow strongly influences the refueling time, with considerable impact on operations. Future work will consider the improved physics of hydrogen and heat transfer, including stratification and refinement of the models; an enhanced simulation environment, considering valves, fuel lines and pumps; inclusion of

airport operational constraints; and consideration of tanks of different size, shape, materials, and insulation type.

Author Contributions: Conceptualization, F.M., D.T. and E.D.B.; methodology, F.M., D.T. and E.D.B.; software, M.Q., F.M. and E.D.B.; validation, M.Q. and E.D.B.; formal analysis, M.Q., F.M. and E.D.B.; investigation, M.Q., F.M. and E.D.B.; resources, M.Q. and E.D.B.; data curation, M.Q. and E.D.B.; writing—original draft preparation, M.Q., F.M. and E.D.B.; writing—review and editing, F.M., M.D.G. and G.A.; visualization, M.Q.; supervision, M.D.G.; project administration, F.M. and D.T.; and funding acquisition, M.D.G., F.M., D.T. and G.A. All authors have read and agreed to the published version of the manuscript.

Funding: The present study was conducted within the Horizon Europe project ALRIGH2T (Grant Agreement no. 101138105), funded by the European Union. Views and opinions expressed are, however, those of the author(s) only and do not necessarily reflect those of the European Union or CINEA. Neither the European Union nor CINEA can be held responsible for them.

Institutional Review Board Statement: Not applicable.

Informed Consent Statement: Not applicable.

Data Availability Statement: The data supporting the conclusions of this article will be made available on request.

Conflicts of Interest: Author Gianvito Apuleo is employed by the company Baykar Piaggio Aerospace S.p.A. The remaining authors declare that the research was conducted in the absence of any commercial or financial relationships that could be construed as a potential conflict of interest.

Abbreviations

The following abbreviations are used in this manuscript:

BOG	Boil-off gas
FL	Filling level
GH2/LH2	Gaseous/Liquid hydrogen
MLI	Multi-layer insulation
SMR	Short–medium-range (aircraft platform)

References

1. Miller, R.; Whittington, E.; Gabra, S.; Hodgson, P.; Green, J.; Kho, J.W.; Smith, J.; Singh, D. Five Years to Chart a New Future for Aviation: The 2030 Sustainable Aviation Goals. In *Aviation Impact Accelerator*; University of Cambridge: Cambridge, UK, 2024. Available online: https://report.aiazero.org/ (accessed on 24 November 2025).
2. ATAG—The Air Transport Action Group. *Beginner's Guide to Sustainable Aviation Fuel*, 4th ed.; 2023. Available online: https://aviationbenefits.org/downloads/beginners-guide-to-sustainable-aviation-fuel/ (accessed on 24 November 2025).
3. EnviroTREC. Liquid Hydrogen for Flight: The Dawn of Zero-Emission Aviation. Available online: https://www.envirotrec.ca/2025/liquid-hydrogen-for-flight-the-dawn-of-zero-emission-aviation/ (accessed on 24 November 2025).
4. Mukhopadhaya, J.; Rutherford, D. Performance Analysis of Evolutionary Hydrogen-Powered Aircraft. International Council on Clean Transportation. 2022. Available online: https://theicct.org/publication/aviation-global-evo-hydrogen-aircraft-jan22/ (accessed on 24 November 2025).
5. EUROCONTROL. Turnaround Time—EUROCONTROL Recommended Values. Available online: https://ansperformance.eu/economics/cba/standard-inputs/latest/chapters/turnaround_time.html (accessed on 24 November 2025).
6. Mangold, J.; Silberhorn, D.; Moebs, N.; Dzikus, N.; Hoelzen, J.; Zill, T.; Strohmayer, A. Refueling of LH2 Aircraft—Assessment of Turnaround Procedures and Aircraft Design Implication. *Energies* **2022**, *15*, 2475. [CrossRef]
7. Hawkins, J. How Do Proportional Relief Valves Improve Hydrogen Boil-Off Gas Management? Available online: https://www.parker.com/ae/en/solutions/hydrogen/boil-off-gas.html (accessed on 24 November 2025).
8. Morales-Ospino, R.; Celzard, A.; Fierro, V. Strategies to recover and minimize boil-off losses during liquid hydrogen storage. *Ren. Sust. Energy Rev.* **2023**, *182*, 113360. [CrossRef]
9. ALRIGH2T Project. Available online: https://alrigh2t.eu (accessed on 24 November 2025).

10. Gil-Esmendia, A.; Flores, R.J.; Brouwer, J. Modeling and improving liquid hydrogen transfer processes. *Appl. Energy* **2025**, *390*, 125779. [CrossRef]
11. Kang, B.; Choi, J.; Lim, I.S.; Lim, H.S.; Ahn, M.; Kim, M.S. Integrated thermal modeling and parametric study of liquid hydrogen storage tanks: Effects of insulation design and operating conditions. *Energy* **2025**, *319*, 134869. [CrossRef]
12. Matveev, K.I.; Leachman, J.W. The Effect of Liquid Hydrogen Tank Size on Self-Pressurization and Constant-Pressure Venting. *Hydrogen* **2023**, *4*, 444–455. [CrossRef]
13. Adler, E.J.; Martins, J.R. Energy demand comparison for carbon-neutral flight. *Prog. Aer. Sci.* **2025**, *152*, 101051. [CrossRef]
14. Mendez Ramos, E.D. Enabling Conceptual Design and Analysis of Cryogenic In-Space Vehicles Through the Development of an Extensible Boil-Off Model. Ph.D. Thesis, Georgia Institute of Technology, Atlanta, GA, USA, 2021.
15. Osipov, V.V.; Daigle, M.J.; Muratov, C.B.; Foygel, M.; Smelyanskiy, V.N.; Watson, M.D. Dynamical Model of Rocket Propellant Loading with Liquid Hydrogen. *J. Spacecr. Rocket.* **2011**, *48*, 987–998. [CrossRef]
16. Daigle, M.J.; Smelyanskiy, V.N.; Boschee, J.; Foygel, M. Temperature Stratification in a Cryogenic Fuel Tank. *J. Thermop. Heat Transf.* **2013**, *27*, 116–126. [CrossRef]
17. Bergman, T. *Fundamentals of Heat and Mass Transfer*, 7th ed.; John Wiley & Sons: Hoboken, NJ, USA, 2011.
18. Keller, C.; Cunnington, G.; Glassford, A. *Thermal Performance of Multilayer Insulations*; NASA TR-134477; NASA: Greenbelt, MD, USA, 1974.
19. Wang, Z.; Merida, W. Thermal performance of cylindrical and spherical liquid hydrogen tanks. *Int. J. Hydrogen Energy* **2024**, *53*, 667–683. [CrossRef]

Disclaimer/Publisher's Note: The statements, opinions and data contained in all publications are solely those of the individual author(s) and contributor(s) and not of MDPI and/or the editor(s). MDPI and/or the editor(s) disclaim responsibility for any injury to people or property resulting from any ideas, methods, instructions or products referred to in the content.